

Spherically symmetric solutions of gravitation equations on the background with spatial sections of constant curvature

M.N. Tentyukov

Joint Institute for Nuclear Research, Dubna.

e-mail: tentukov@thsun1.jinr.dubna.su

Abstract

We investigate the vacuum and charged spherically symmetric static solutions of the Einstein equations on cosmological background. The background metric is not flat, but curved, with constant - curvature spatial sections.

Both vacuum and charged cases contain two branches. The first branches transform into the Schwarzschild and Reissner-Nordström solutions if the background metric goes to the Minkovski one. The second branches describe wormholes and have no Einstein limit.

1 Introduction

It is well - known that the equations describing gravitation with a given background metric coincide with the Einstein ones if the background metric satisfies the "background" Einstein equations [1]. However, if the background metric is arbitrary, the gravitational equations differ from the Einstein equations. Some exact solutions of these equations which are in form very close to the Einstein solutions acquire new specific features.

There are at least two reasons for these solutions to be interesting.

First, they are solutions of the Einstein equations on the nontrivial cosmological background. That is why they may be physically meaningful in the early Universe.

When the quantum properties of gravity were important, the Einstein theory was to be replaced by the effective theory that includes quantum effects. Later on, gravitation was described by the Einstein equations. However, the intermediate period between quantum and Einstein states may admit the description in terms of the Einstein gravity on the quantum - corrected background.

Solutions on the nontrivial background may be useful for the functional integral approach to quantum gravity. In the semiclassical approximation, the dominant contribution to the path integral will come from the neighborhood of saddle points of the action, that is, of classical solutions. It seems to be interesting to compare the path integral based on the Gibbos - Hawking action with another model, whose properties may be different.

Of course, we can write down any metric which does not satisfy any equations. However, to derive the Lagrangian is a more complicated problem. Indeed, R is the only scalar without essential higher derivatives. All other Lagrangians contain either higher derivatives or additional dynamical degrees of freedom.

Introducing a nondynamical background object, we can derive solutions with very different properties and, at the same time, retain the basic structure of the Lagrangian.

2 Basic results

In the present paper, we consider the gravitation described by the spherically symmetric static metric

$$ds^2 = g_{ik} dx^i dx^k$$

on the background

$$d\tilde{s}^2 = dt^2 - dr^2 - k^2 \sinh^2 \frac{r}{k} d\Omega, \quad (1a)$$

where $d\Omega = (d\theta^2 + \sin^2 \theta d\phi^2)$. The spatial sections $t = \text{const}$ are 3-d Lobachevski spaces (a constant negative curvature space of radius k). For simplicity, we use the system of units $\hbar = c = G = k_\beta = 1$. It is convenient to shift a coordinate r to some value r_0 so that (1a) takes the form

$$d\tilde{s}^2 = dt^2 - dr^2 - k^2 \sinh^2 \frac{r - r_0}{k} d\Omega. \quad (1b)$$

The equations

$$R_{ij} - \check{R}_{ij} = 8\pi(T_{ij} - \frac{1}{2}g_{ij}T), \quad (2)$$

where \check{R}_{ij} is the background Ricci tensor, T_{ij} is the energy - momentum tensor of the external matter, are derived from the action

$$S = \int (L_g + L_M) d^4x$$

with the Rosen [2] gravitational Lagrangian

$$L_g = \sqrt{-g} g^{mn} (P_{mb}^a P_{an}^b - P_{sa}^a P_{mn}^s). \quad (3)$$

Here the affine - deformation tensor

$$P_{jk}^i = \check{\Gamma}_{jk}^i - \Gamma_{jk}^i$$

is the difference between the background connection and the Levi - Chivita connection for physical metric. The matter Lagrangian L_M does not contain background objects.

We will investigate the vacuum (5) and charged (8) spherically symmetric static solutions of equations (2). Both the cases contain two branches. The first branches (6) and (9) transform into the Schwarzschild and Reissner-Nordström solutions if we put $k \rightarrow \infty$. The second branches (7) and (12) describe wormholes and have no Einstein limit (they diverge when $k \rightarrow \infty$).

A charged wormhole can contain an event horizon and the Cauchy horizon in the throat. Then structure of the whole geodesic space - time is similar to the Kerr solution. It is interesting that the corresponding black holes have a positive heat capacity.

Equations (2) on the background (1) were considered for a localized mass [3] and the electric charge [4]. If we put $k \rightarrow \infty$, the metric (1) goes over to the Minkowski metric, and equations (2) turn into the Einstein equations.

Arbitrary spherically symmetric static metric may be written in the form

$$ds^2 = \Lambda(r)dt^2 - \frac{1}{\Lambda(r)}dr^2 - R^2d\Omega^2. \quad (4)$$

The causal structure of space - time is determined by the metric function Λ , and $R(r)$ is the "luminosity" distance. It may be shown that, if $R(r)$ is an increasing function, the decreasing function Λ describes repulsion of a test body from the central source; while increasing Λ , attraction.

Let us denote

$$\begin{aligned} \Lambda_1 &= \exp(2r_0/k) \frac{\sinh \frac{r-2r_0}{k}}{\sinh \frac{r}{k}}, \\ \Lambda_2 &= \exp(2r_0/k) \frac{\cosh \frac{r-2r_0}{k}}{\cosh \frac{r}{k}}, \\ R_1 &= \exp(-r_0/k) k \sinh \frac{r}{k}, \\ R_2 &= \exp(-r_0/k) k \cosh \frac{r}{k}. \end{aligned}$$

First of all we consider the vacuum case $T_{ij} = 0$:

$$R_{ij} = \check{R}_{ij}. \quad (5)$$

Besides the solution

$$ds_{V1}^2 = \Lambda_1 dt^2 - \frac{1}{\Lambda_1} dr^2 - R_1^2 d\Omega^2 \quad (6)$$

transforming to the Schwarzschild solution when $k \rightarrow \infty$ there is the second solution of (5)

$$ds_{V2}^2 = \Lambda_2 dt^2 - \frac{1}{\Lambda_2} dr^2 - R_2^2 d\Omega^2 \quad (7)$$

describing traversible wormhole. This second branch demands nontrivial background topology continued to negative r .

The solution (6) was found in [3]. It contains a Schwarzschild - like singularity on the event horizon at $r = 2r_0$. The metric function and the luminosity distance are shown in fig.1.

We may find the coordinate system in which (6) is regular at $r = 2r_0$ but in these coordinates there is the background metric (1) singularity. Since the background metric is non - observable, we are interested only in the physical metric (6). The causal structure of maximal analytic extension (6) is the same as the Schwarzschild one. Note that if $r_0 \ll k$, the value of r_0 is very close to the value of mass of the central source. If $r_0 \rightarrow 0$, then (6) goes over to the background metric (1). The asymptotics of (6) for $r \rightarrow \infty$ coincides with the asymptotics of (1b).

The metric function of (7) is regular at all r and the luminosity distance has a minimum at $r = 0$ (see fig.2). It means that if r is smaller than r_0 , the metric (7) describes a traversible wormhole. The locally defined background (1) derives locally the physical metric (7) by means of equations (5). The geodesic completeness of (7) leads to the topology both of background and physical metrics.

Solution (7) diverges if $k \rightarrow \infty$ because the minimum of $R_2(r)$ goes to ∞ . Asymptotics of (7) for $r \rightarrow \infty$ is the same as that of (6) and (1b) but if $r_0 \rightarrow 0$, the metric (7) turns to the metric

$$ds^2 = dt^2 - dr^2 - k^2 \cosh^2 \frac{r}{k} d\Omega^2$$

describing a symmetric wormhole in the absolute empty space.

If $r_0 > 0$, the asymptotics of the physical metric for $r \rightarrow -\infty$ differs from the background one. It can be shown that the wormhole sucks in a matter from the 3-space with a nonbackground asymptotics and then throws out it into the 3-space whose asymptotics is the same as the background one. However, a rapidly moving radial observer can visit another 3-space and then return to his home during a finite proper time.

Now let us consider equations (2) with the energy - momentum tensor of a localized electric charge Q :

$$R_{ij} - \check{R}_{ij} = 8\pi T_{Qij}. \quad (8)$$

Here we also obtain two branches. The first

$$ds_{Q1}^2 = \Lambda_{Q1} dt^2 - \frac{1}{\Lambda_{Q1}} dr^2 - R_1^2 d\Omega^2, \quad (9)$$

where

$$\Lambda_{Q1} = \Lambda_1 + \exp\left(\frac{4r_0}{k}\right) \frac{Q^2}{k^2} \sinh^{-2} \frac{r}{k}$$

was found in [4]. When $k \rightarrow \infty$, it passes into the Reissner-Nordström solution. If $Q = 0$, then (9) coincides with (6). If $Q < Q_{10}$, where

$$Q_{10} = \frac{k \sinh \frac{r_0}{k}}{\sinh \frac{r_0}{k} + \cosh \frac{r_0}{k}}, \quad (10)$$

there are two horizons at r_{1+} and r_{1-} ,

$$r_{1\pm} = r_0 \pm k \operatorname{arcsinh} \sqrt{\sinh^2 \frac{r_0}{k} - \frac{Q^2}{k^2} \left(\sinh \frac{r_0}{k} + \cosh \frac{r_0}{k} \right)^2}. \quad (11)$$

When $Q > Q_{10}$, horizons are absent. If $Q = Q_{10}$, the horizons merge into a single horizon at $r = r_0$ and an extreme black hole forms.

The second branch

$$ds_{Q2}^2 = \Lambda_{Q2} dt^2 - \frac{1}{\Lambda_{Q2}} dr^2 - R_2^2 d\Omega^2, \quad (12)$$

where

$$\Lambda_{Q2} = \Lambda_2 - \exp\left(\frac{4r_0}{k}\right) \frac{Q^2}{k^2} \cosh^{-2} \frac{r}{k},$$

should be interpreted similarly to the metric (7).

If $Q = 0$, then (9) coincides with (7). If $Q < Q_{20}$, where

$$Q_{20} = \frac{k \cosh \frac{r_0}{k}}{\sinh \frac{r_0}{k} + \cosh \frac{r_0}{k}}, \quad (13)$$

metric (12) describes the traversible wormhole. If $Q = Q_{20}$, there is a horizon in the throat. When $Q > Q_{10}$, there are two horizons at r_{2+} and r_{2-} ,

$$r_{2\pm} = r_0 \pm k \operatorname{arcsinh} \sqrt{-\cosh^2 \frac{r_0}{k} + \frac{Q^2}{k^2} \left(\sinh \frac{r_0}{k} + \cosh \frac{r_0}{k} \right)^2}. \quad (14)$$

Note that from (10) and (13) we have

$$Q_{10} = Q_{20} \tanh \frac{r_0}{k}.$$

Since $\tanh \frac{r_0}{k} < 1$, we have $Q_{10} < Q_{20}$. Because in (9) a horizon exists if $Q < Q_{10}$, and in (12) it exists if $Q > Q_{20}$, for any r_0 there is an area of Q in which there are horizons neither in (9) nor in (12).

Now we return to solution (12).

When $Q = \lim_{r_0 \rightarrow 0} Q_{20} = k$, horizons depend on r_0 as shown in fig.3. If $Q < k$, for small enough r_0 a horizon is absent. If $Q > k$, then even for $r_0 = 0$ there are two horizons at $r_{2\pm\min} = \pm k \operatorname{arcsinh} \sqrt{\frac{Q^2}{k^2} - 1}$ (fig.4).

When there are two horizons, the causal structure of (12) is similar to the Kerr solution but without singularity. The conformal diagram is shown in fig.5.

Temperature of the solutions with horizons can be found by investigating the Euclidean sections of the corresponding metrics [5].

For (6) and (9) the corresponding temperatures are

$$T_{V1} = \frac{\exp\left(\frac{2r_0}{k}\right)}{4\pi k} \frac{1}{\sinh \frac{2r_0}{k}} = \frac{1}{4\pi k} \left(1 + \tanh^{-1}\left(\frac{2r_0}{k}\right)\right) \quad (15)$$

$$T_{Q1} = \frac{\exp\left(\frac{2r_0}{k}\right)}{4\pi k} \frac{\sinh \frac{r_{1+}-r_{1-}}{k}}{\sinh^2 \frac{r_{1+}}{k}} \quad (16)$$

The dependence of T_{Q1} on r_0 is very close to the dependence of T_{V1} , if r_0 is not very small. If $k \rightarrow \infty$, then (15) and (16) pass into expressions for temperatures of the Schwarzschild and Reissner-Nordström solution, respectively. When $r_0 \rightarrow 0$, then $T_{V1} \rightarrow \infty$ as the Schwarzschild temperature. The behavior of T_{V1} is similar, but when r_0 is very small, then for any (small) Q the horizon does not form, and at $Q = Q_{10}$ the temperature $T_{Q1} = 0$. That is why for any $Q \neq 0$ there is a neighborhood of 0 for r_0 in which T_{V1} and T_{Q1} depend on r_0 as shown in fig.6.

For large r_0 the situation differs from the GR one:

$$\lim_{r_0 \rightarrow \infty} T_{V1} = \lim_{r_0 \rightarrow \infty} T_{Q1} = \frac{1}{2\pi k}.$$

It means that very heavy black holes can't have temperature less than $\frac{1}{2\pi k}$.

The solution (12) has two temperatures. In the 3-space when r_{2+} is the event horizon and r_{2-} is the Cauchy horizon, we observe the temperature

$$T_{Q2+} = \frac{\exp\left(\frac{2r_0}{k}\right)}{4\pi k} \frac{\sinh \frac{r_{2+}-r_{2-}}{k}}{\cosh^2 \frac{r_{2+}}{k}}, \quad (17)$$

and in the 3-space, when r_{2-} is the event horizon and r_{2+} is the Cauchy horizon, we observe the temperature

$$T_{Q2-} = \frac{1}{4\pi k} \frac{\sinh \frac{r_{2+}-r_{2-}}{k}}{\cosh^2 \frac{r_{2-}}{k}}. \quad (18)$$

These temperatures are increasing functions of r_0 ! Therefore, the heat capacity of (12) is positive definit, and so we can use a normal canonical ensemble. The lower limit for both the temperatures is equal to

$$l = \frac{\sqrt{1 - \frac{k^2}{Q^2}}}{2\pi k}. \quad (19)$$

The maximal value of T_{Q2+} is $\frac{1}{2\pi k}$, and the maximal value of T_{Q2-} is

$$L = \frac{\left(1 - 4\frac{Q^2}{k^2}\right)^2}{32\pi k \frac{Q^4}{k^4}} \quad (20)$$

From (19) we can see that for $Q = k$ the minimal of temperature is zero, and if $Q > k$, then the minimal temperature is large than zero. When $Q < k$, then horizons will form only if r_0 is not very small, and the lower temperature corresponds to the minimal value of r_0 obtained from (13):

$$r_{0\min} = k \operatorname{arctanh} \frac{k - Q}{Q}.$$

3 Causal structure of the vacuum solution

Let us consider the common metric (4) and go to the coordinates U, V :

$$\begin{cases} t + f(r) &= U, \\ t - f(r) &= V. \end{cases}$$

If $\Lambda f'^2 = \frac{1}{\Lambda}$, that is

$$f = \pm \int \frac{dr}{\Lambda}, \quad (21)$$

then U and V are null coordinates and the metric (4) takes the form

$$ds^2 = \Lambda dU dV + R^2 d\Omega^2.$$

We are interested in the case when $d\Omega = 0$, so,

$$ds^2 = \Lambda dU dV. \quad (22)$$

At a horizon we have $\Lambda = 0$. To avoid this peculiarity, we can attempt to perform the coordinate transformation $\tilde{U} = \tilde{U}(U)$, $\tilde{V} = \tilde{V}(V)$ so that

$$ds^2 = \frac{\Lambda}{\frac{d\tilde{U}}{dU} \frac{d\tilde{V}}{dV}} d\tilde{U} d\tilde{V}. \quad (23)$$

If $\frac{d\tilde{U}}{dU} \frac{d\tilde{V}}{dV}$ at a horizon has the same peculiarity as Λ , then the metric (23) becomes regular.

For the metric (6) we have

$$f = A \left(Br + \ln \left| \sinh \frac{r - 2r_0}{k} \right| \right),$$

where $B = \frac{1}{k} \tanh^{-1} \left(\frac{2r_0}{k} \right)$, $A = \frac{k}{1+kB}$. In the coordinates

$$\begin{cases} \tilde{U} &= \exp \left(\frac{U}{2A} \right), \\ \tilde{V} &= -\exp \left(-\frac{V}{2A} \right), \end{cases} \quad (24)$$

we get the metric(6) in the form (23):

$$ds_{V1}^2 = 4A^2 \exp \left(\frac{2r_0}{k} \right) \frac{1}{\sinh \frac{r}{k} \exp(Br)} d\tilde{U} d\tilde{V}.$$

. The conformal diagram constructed similarly to the Schwarzschild one.

4 The wormhole

Although the coordinate r in (1b) changes only in the area $r_0 < r < \infty$, we can formally consider continuation of the functions $\Lambda(r)$ and $R(r)$ onto all the real numbers $-\infty < r < \infty$.

Now let us consider the solution (7).

As we can see from fig.2, the metric (7) describes gravitational repulsion if $r > 0$. The space - time described by (7) is regular at all r . Test particles can cross the sphere $r = 0$ and reach negative values of r . Actually, (7) contains the traversible wormhole at $r = 0$ connecting two infinitely 3-spaces $r < r_0$ and $r > r_0$. For this interpretation, we must extend the background (1b) to the area $r < r_0$ (or (1a) to $r < 0$) and consider the background space as two the Lobachevsky spaces glued at $r = 0$.

On this background, the solution (7) of equations (5) is defined at $-\infty < r < \infty$. For investigation of the region with $r < r_0$, we can do the following coordinate and constant transformations:

$$\begin{aligned} \tilde{r} &= -r \exp \left(-\frac{2r_0}{k} \right); & \tilde{t} &= t \exp \left(\frac{2r_0}{k} \right); \\ \tilde{k} &= k \exp \left(-\frac{2r_0}{k} \right); & \tilde{r}_0 &= r_0 \exp \left(-\frac{2r_0}{k} \right). \end{aligned} \quad (25)$$

Note that $\tilde{r}_0/\tilde{k} = r_0/k$, $k > \tilde{k}$. The metric (7) takes the form

$$d\tilde{s}_{V2}^2 = \tilde{\Lambda}_2 d\tilde{t}^2 - \frac{1}{\tilde{\Lambda}_2} d\tilde{r}^2 - \tilde{R}_2^2 d\Omega^2, \quad (26)$$

where

$$\tilde{\Lambda}_2 = \exp \left(-\frac{2\tilde{r}_0}{\tilde{k}} \right) \frac{\cosh \frac{\tilde{r}+2\tilde{r}_0}{\tilde{k}}}{\cosh \frac{\tilde{r}}{\tilde{k}}}, \quad \tilde{R}_2 = \exp \left(\tilde{r}_0/\tilde{k} \right) \tilde{k} \cosh \frac{\tilde{r}}{\tilde{k}}.$$

Asymptotics (26) for $\tilde{r} \rightarrow \infty$ coincides with the asymptotics of the Lobachevski space with radius \tilde{k} . To make this clear, we should pass to the coordinate $\rho = \tilde{r} + \tilde{r}_0$. If $\tilde{r} > 0$, the metric (26) describes gravitational

attraction. In fig.8 it is shown conditional representation of the space-time of the wormhole. In fig.8 we can see the embedding diagram which is two dimensional model of the spatial section at a specific moment of time, embedded into a fictitious 3 - dimensional space. Note that the background topology differs from the physical one. A continuous line in the background space corresponds to the discontinuity of the physical line at $r = r_0$. To avoid this phenomenon, we should further change the background topology and consider the background 3-space as a limit when $\varepsilon \rightarrow 0$ of two spatial sections (1b) glued on the sphere $r_0 + \varepsilon$ (fig.7).

5 Radial geodesics

Equations of geodesics can be obtained from the Lagrangian

$$L = \frac{1}{2}g_{ij}\dot{x}^i\dot{x}^j,$$

where \dot{x} means $\frac{d}{d\tau}$ and τ is a proper time [6]. For radial geodesics in the metric (4) this Lagrangian takes the form

$$L = \frac{1}{2} \left(\Lambda \dot{t}^2 - \frac{1}{\Lambda} \dot{r}^2 \right). \quad (27)$$

The Euler equation for (27) is

$$\frac{d}{d\tau}(\Lambda \dot{t}) = 0.$$

From this formula we get $\dot{t}^2 = \frac{D^2}{\Lambda^2}$, where $D = \text{const}$ is a constant of motion. Let us substitute it into (27) and take into account that $\dot{x}^i\dot{x}^j g_{ij} = 1$. We obtain

$$\Lambda + v^2 = D^2, \quad (28)$$

where $v = \dot{r}$. Consequently, the proper time of radial motion from the point with coordinate r_1 to the point with coordinate r_2 is

$$\tau_{12} = \pm \int_{r_1}^{r_2} \frac{dr}{\sqrt{D^2 - \Lambda(r)}}.$$

Since direction of motion is towards the center we have for $r_1 > r_2$ that $\tau_1 < \tau_2$. Finally, the proper time of radial motion from r_1 to r_2 is

$$\Delta\tau = \int_{r_2}^{r_1} \frac{dr}{\sqrt{D^2 - \Lambda}}. \quad (29)$$

Let us consider a free falling body in the metric (9) with the parabolic velocity $\lim_{r \rightarrow \infty} v = 0$. From (28) we get $D_1^2 = 1$. Let

$$\begin{aligned} T_1(r) &= \int \frac{dr}{\sqrt{1-\Lambda_1}} = \\ &= \frac{k}{\sqrt{\exp(\frac{4r_0}{k})-1}} \left(\sqrt{\exp\left(\frac{2r}{k}\right)-1} - \operatorname{arctg} \sqrt{\exp\left(\frac{2r}{k}\right)-1} \right). \end{aligned} \quad (30)$$

From(29) we obtain the proper time of free fall from $r = r_i$ to $r = r_f < r_i$:

$$\Delta\tau = T_1(r_i) - T_1(r_f).$$

From (30) we can see that $\Delta\tau$ diverges when $r_i \rightarrow \infty$ but it is finite for any other r_i and r_f .

Now let us consider the fall in metric (7). In this case we cannot assume $v \rightarrow 0$ when $r \rightarrow \infty$ because test bodies are repulsed by the center. That is why we put $v = 0$ at $r = -\infty$:

$$D_2^2 = \lim_{r \rightarrow -\infty} \Lambda_2 = \exp\left(\frac{4r_0}{k}\right).$$

From(29) we obtain the proper time of free fall from $r = r_i$ to $r = r_f < r_i$:

$$\Delta\tau = T_2(r_i) - T_2(r_f),$$

where

$$\begin{aligned} T_2(r) &= \\ &= \frac{k}{\sqrt{\exp(\frac{4r_0}{k})-1}} \left(-\sqrt{\exp\left(-\frac{2r}{k}\right)+1} - \frac{1}{2} \ln \frac{\sqrt{\exp\left(-\frac{2r}{k}\right)+1}-1}{\sqrt{\exp\left(-\frac{2r}{k}\right)+1}+1} \right). \end{aligned} \quad (31)$$

It is clear from (31) that $\Delta\tau$ is finite for all finite r_i and r_f and diverges both for $r_i \rightarrow \infty$ (ln) and for $r_f \rightarrow -\infty$ (the first term in the brackets).

6 The metric functions of the charged solution

Sets of the metric functions (9) and (12) for different Q are shown in fig.10 and fig.11, respectively.

If $Q \leq Q_{10}$ (see (10)), then the metric function Λ_{Q1} may be represented in the form

$$\Lambda_{Q1} = \exp\left(\frac{2r_0}{k}\right) \frac{\sinh\left(\frac{r-r_{1-}}{k}\right) \sinh\left(\frac{r-r_{1+}}{k}\right)}{\sinh^2 \frac{r}{k}}, \quad (32)$$

with the horizons

$$r_{1\pm} = r_0 \pm k\Delta_1. \quad (33)$$

Here Δ_1 can be derived by the following formulas:

$$\sinh \Delta_1 = \sqrt{\sinh^2 \frac{r_0}{k} - \frac{Q^2}{k^2} \left(\sinh \frac{r_0}{k} + \cosh \frac{r_0}{k} \right)^2} \quad (34)$$

or

$$\cosh \Delta_1 = \sqrt{\cosh^2 \frac{r_0}{k} - \frac{Q^2}{k^2} \left(\sinh \frac{r_0}{k} + \cosh \frac{r_0}{k} \right)^2}. \quad (35)$$

The metric function Λ_{Q2} has a similar representation:

$$\Lambda_{Q2} = \exp \left(\frac{2r_0}{k} \right) \frac{\sinh \left(\frac{r-r_{2-}}{k} \right) \sinh \left(\frac{r-r_{2+}}{k} \right)}{\sinh^2 \frac{r}{k}}, \quad (36)$$

where

$$r_{2\pm} = r_0 \pm k\Delta_2, \quad (37)$$

and

$$\sinh \Delta_2 = \sqrt{-\cosh^2 \frac{r_0}{k} + \frac{Q^2}{k^2} \left(\sinh \frac{r_0}{k} + \cosh \frac{r_0}{k} \right)^2} \quad (38)$$

or

$$\cosh \Delta_2 = \sqrt{-\sinh^2 \frac{r_0}{k} + \frac{Q^2}{k^2} \left(\sinh \frac{r_0}{k} + \cosh \frac{r_0}{k} \right)^2}. \quad (39)$$

7 Causal structure of charged solutions

For transition to the coordinates (22) we need the function f (21). We are interested in solutions with horizons, therefore, metric functions may be taken in the form (32) and (36). The corresponding integrals can be easily calculated. The forms for both the functions are the same up to constants:

$$f = Ar + B \ln \left| \sinh \frac{r-r_-}{k} \right| + C \ln \left| \sinh \frac{r-r_+}{k} \right|.$$

For the metric (9)

$$\begin{aligned} A_1 &= \exp \left(-\frac{2r_0}{k} \right) \cosh \frac{r_{1-} + r_{1+}}{k}; & B_1 &= -\exp \left(-\frac{2r_0}{k} \right) \frac{k \sinh^2 \frac{r_{1-}}{k}}{\sinh \frac{r_{1+} - r_{1-}}{k}}; \\ C_1 &= -\exp \left(-\frac{2r_0}{k} \right) \frac{k \sinh^2 \frac{r_{1+}}{k}}{\sinh \frac{r_{1+} - r_{1-}}{k}}; & r_- &= r_{1-}; \quad r_+ = r_{1+}, \end{aligned}$$

and for the metric(12)

$$\begin{aligned} A_2 &= \exp \left(-\frac{2r_0}{k} \right) \cosh \frac{r_{2-} + r_{2+}}{k}; & B_2 &= -\exp \left(-\frac{2r_0}{k} \right) \frac{k \sinh^2 \frac{r_{2-}}{k}}{\sinh \frac{r_{2+} - r_{2-}}{k}}; \\ C_2 &= -\exp \left(-\frac{2r_0}{k} \right) \frac{k \sinh^2 \frac{r_{2+}}{k}}{\sinh \frac{r_{2+} - r_{2-}}{k}}; & r_- &= r_{2-}; \quad r_+ = r_{2+}. \end{aligned}$$

Now we can go to the coordinates in which metrics are regular at r_+ :

$$\tilde{U} = \exp\left(\frac{U}{2C}\right); \quad \tilde{V} = -\exp\left(-\frac{V}{2C}\right).$$

Similar coordinates can be constructed to avoid coordinate singularity at r_- :

$$\tilde{U} = \exp\left(\frac{U}{2B}\right); \quad \tilde{V} = -\exp\left(-\frac{V}{2B}\right).$$

The conformal diagram for (9) is similar to the Reissner-Nordström solution. Because of a time-like singularity at $r = 0$ we cannot continue the space-time to the negative value of r .

The conformal diagram for solution (12) differs from the previous one by absence of singularities. In principle, the conformal diagram is very close to the diagram of the Kerr solution (fig.5).

In domain I the physical 3-space asymptotically turns into the background when $r \rightarrow \infty$. In domain II we may perform the coordinate transformation similar to (25):

$$\begin{aligned} \tilde{r} &= -r \exp\left(-\frac{2r_0}{k}\right); & \tilde{t} &= t \exp\left(\frac{2r_0}{k}\right); \\ \tilde{k} &= k \exp\left(-\frac{2r_0}{k}\right); & \tilde{r}_0 &= r_0 \exp\left(-\frac{2r_0}{k}\right); \\ \tilde{r}_{2+} &= -r_{2-} \exp\left(-\frac{2r_0}{k}\right); & \tilde{r}_{2-} &= -r_{2+} \exp\left(-\frac{2r_0}{k}\right). \end{aligned} \quad (40)$$

Then the metric (12) can be written as

$$d\tilde{s}_{Q2}^2 = \tilde{\Lambda}_{Q2} d\tilde{t}^2 - \frac{1}{\tilde{\Lambda}_{Q2}} d\tilde{r}^2 - \exp\left(\frac{2\tilde{r}_0}{\tilde{k}}\right) \tilde{k}^2 \cosh^2 \frac{\tilde{r}}{\tilde{k}} d\Omega^2, \quad (41)$$

where

$$\tilde{\Lambda}_{Q2} = \exp\left(-\frac{2\tilde{r}_0}{\tilde{k}}\right) \frac{\sinh\left(\frac{\tilde{r}}{\tilde{k}} - \frac{\tilde{r}_{2+}}{\tilde{k}}\right) \sinh\left(\frac{\tilde{r}}{\tilde{k}} - \frac{\tilde{r}_{2-}}{\tilde{k}}\right)}{\cosh^2 \frac{\tilde{r}}{\tilde{k}}}. \quad (42)$$

It is clear that now \tilde{r}_{2+} is the event horizon, and \tilde{r}_{2-} is the Cauchy horizon. Note that the asymptotics of the 3-space in domain II is the Lobachevski space with the curvature radius $\tilde{k} \neq k$! Since r_{2+} and r_{2-} have opposite signs, the throat $r = 0$ is spacelike. If observer goes from domain I into domain III and crosses the horizon r_{2+} , then he must fall through the wormhole, but he may choose where he appears after that between two symmetric domains II and II'. Actually, we have two enumerable sets of wormholes.

8 Temperature of the solution with horizons

The Euclidean section of metric (4) is

$$ds^2 = \Lambda d\tau^2 + \frac{1}{\Lambda} dr^2 + R^2 d\Omega^2.$$

This metric is regular on the horizon [5], if the euclidean time τ is periodic $0 \leq \tau \leq \beta$ with the period

$$\beta = \frac{4\pi}{\frac{d}{dr}\Lambda}\Big|_{r=r_+}$$

. The corresponding temperature appears to be

$$T = \beta^{-1} = \frac{1}{4\pi} \frac{d}{dr}\Lambda\Big|_{r=r_+}. \quad (43)$$

By substituting the corresponding values of Λ into this formula we obtain the temperature T_{V1} (15) for the metric (6), the temperature T_{Q1} (16) for the metric (9) and the temperature T_{Q2+} (17) for the metric (12). We cannot obtain the temperature T_{Q2-} by substituting r_- instead of r_+ into (43) because in domain III r_- is not the event horizon, it is the Cauchy horizon. This temperature is observed in domain II, where r_{2-} is the event horizon. To obtain it, we may substitute the metric function Λ_{Q2} (42) into (43). The resulting expression is (18).

The asymptotics are easily calculated by using the follow formulas:

$$\begin{aligned} \tanh \Delta_1 &= \tanh\left(\frac{r_0}{k}\right) \sqrt{\frac{1 - \frac{Q^2}{k^2} \left(1 - \tanh^{-1}\left(\frac{r_0}{k}\right)\right)^2}{1 - \frac{Q^2}{k^2} \left(1 - \tanh\left(\frac{r_0}{k}\right)\right)^2}}, \\ \tanh \Delta_2 &= \tanh^{-1}\left(\frac{r_0}{k}\right) \sqrt{\frac{\frac{Q^2}{k^2} \left(1 - \tanh\left(\frac{r_0}{k}\right)\right)^2 - 1}{\frac{Q^2}{k^2} \left(1 - \tanh^{-1}\left(\frac{r_0}{k}\right)\right)^2 - 1}}. \end{aligned}$$

These formulas may be obtained from (34, 35) and (38, 39).

9 Conclusion

Within the context of a spherically symmetric model in the presence of a nontrivial background we have investigated some exact solutions of gravitation equations. We have found that there are two branches of the solutions. The first branch is close to the corresponding solution of the Einstein equation, and the second has a set of nontrivial properties and diverges if the background passes into the Minkovski space.

It is worth noting that the second branches should be of essentially cosmological origin because the radius of wormholes is equal to the Universe radius k .

In principle, this toy model may be considered as a very anisotropic cosmological model, in which both local and global properties are described by the gravitational field produced by the central-symmetric solution.

The first cosmological model was a static cylinder Universe. After discovering the cosmological redshift it became clear that the observed Universe should be nonstationary.

However, in principle, "scattering" of the Galaxies can be understood in the framework of a static cosmology.

Let us suppose that the Einstein cylinder is actually a throat of the wormhole with cosmological radius. If the metric is such that the test bodies are attracted by the throat from one side and repulsed from another, then it is clear that close to the minimal radius, the local metric appears to be nonstationary for a free falling observer.

Such a model is impossible in the framework of the conventional General Relativity because the violation of energy conditions is necessary for the wormhole creation [7]. If we consider the gravitation on the nontrivial cosmological background, similar solutions can appear.

Much attention has been paid to the investigation of wormholes. Classical wormholes usually are Euclidean metrics which consist of two large regions of spacetime connected by a throat. They play an important role in quantum gravity [8, 9]. It was just the microscopic wormholes which have a Planck size throat. An analytic continuation of closed cosmological solutions to imaginary time leads to euclidean wormholes with the size of the throat equal to the maximum size of the universe [10]. Wormholes considered in the present paper demonstrate similar properties but in the Lorentzian sections.

References

- [1] Grischuk L.P., Petrov A.N., Popova A.D. *Comm. Math. Phys.* **94** (1984) 379.
- [2] Rosen N. *Found. Phys.* **10** (1980) 673.
- [3] Chernikov N.A. *Acta Phys. Pol.B.* **24** (1993) 927.
- [4] Asanov R.A. *Found. Phys.* **25** (1995) 949.
- [5] Gibbons C.W., Hawking S.W. *Phys. Rev.* **D15** (1977) 2752.
- [6] Chandrasekhar S. *The mathematical theory of black holes* – Clarendon Press Oxford, Oxford Univ. Press, New York, 1983.
- [7] Morris M.S., Thorne K.S., Yurtsever U. *Phys. Rev. Lett.* **61** (1988) 1446.
- [8] Hawking S. W. *Mod. Phys. Lett.* **A5** (1990) 145.
- [9] Hawking S. W. *Mod. Phys. Lett.* **A5** (1990) 453.

[10] Zhuk A. *Phys. Lett.* **A176** (1993) 176.

Figure Captions

Figure 1. The metric function and luminosity distance for the metric (6); the dashed curve shows Λ^{-1} .

Figure 2. The metric function and luminosity distance for the metric (7).

Figure 3. Horizons of the metric (12).

Figure 4. A minimal possible value of the horizon for metric (12).

Figure 5. Conformal diagram for the solution (12).

Figure 6. Temperatures of the metrics (6) and (9); $r_{0\min} = k \operatorname{arctanh} \frac{Q}{k-Q}$.

Figure 7. Spatial sections of the background metric embedded into a fictitious high - dimensional space.

Figure 8. Conditional representation of the space - time of the wormhole.

Figure 9. Spatial sections of the physical metric. The background metric is also shown. Continuous line in the background space corresponds to the discontinuity of the physical line at $r = 0$.

Figure 10. The metric function for the metric(9) for different values of Q .

Figure 11. The metric function for the metric(12) for different values of Q .

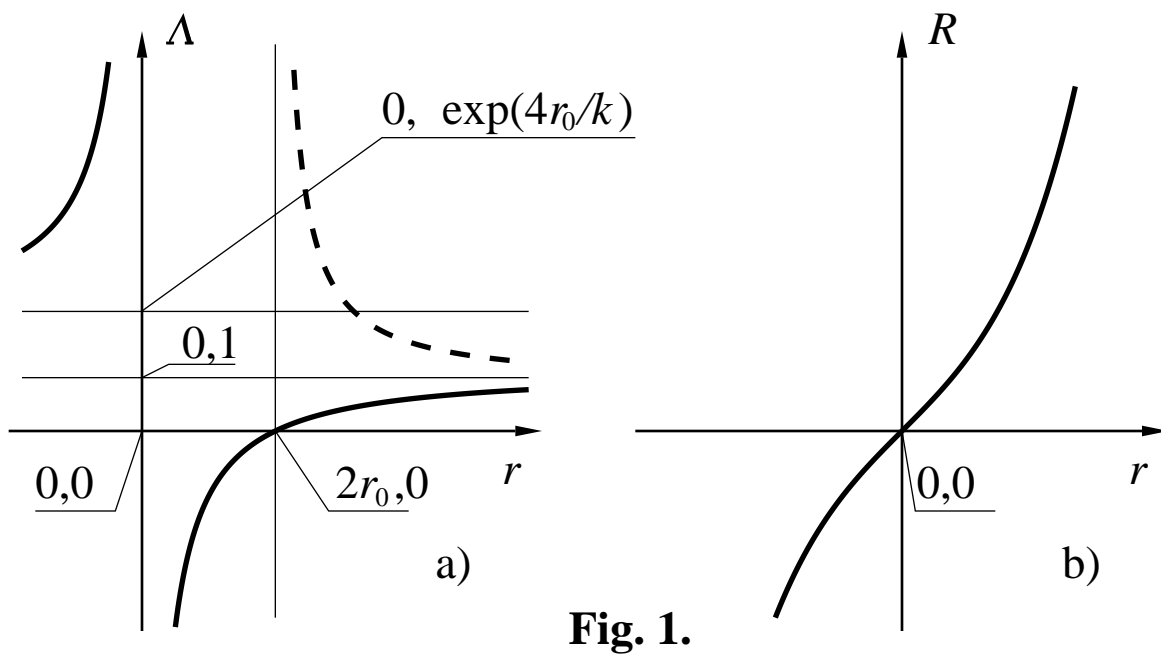


Fig. 1.

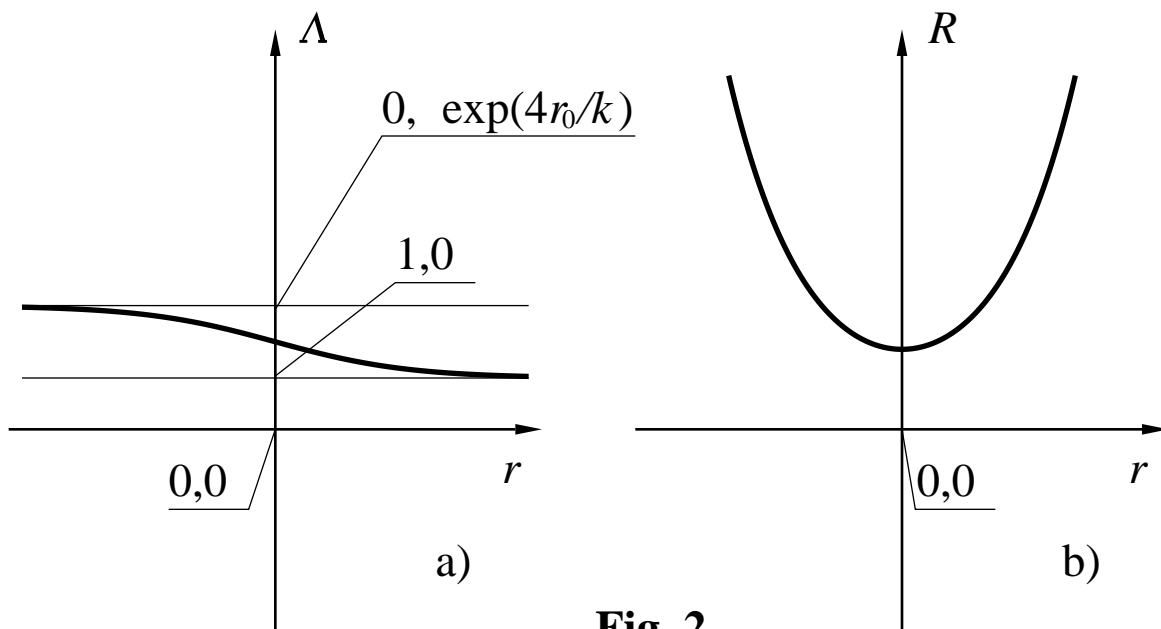


Fig. 2.

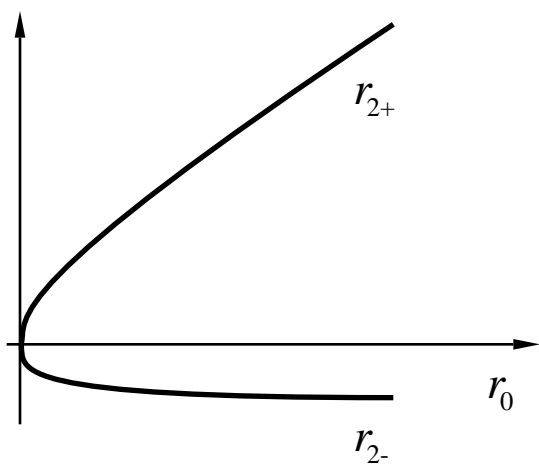


Fig. 3.

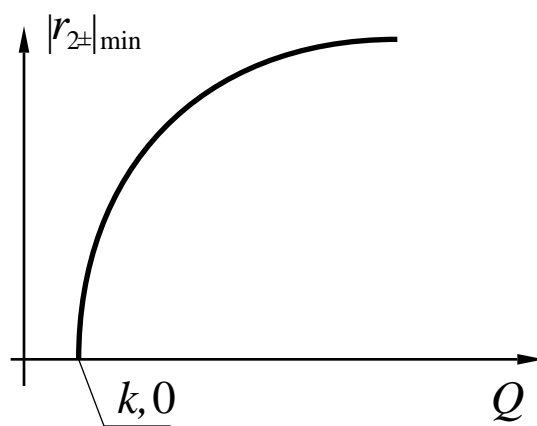


Fig. 4.

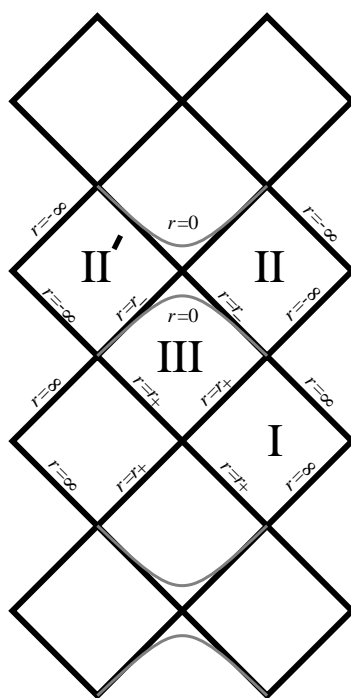


Fig. 5.

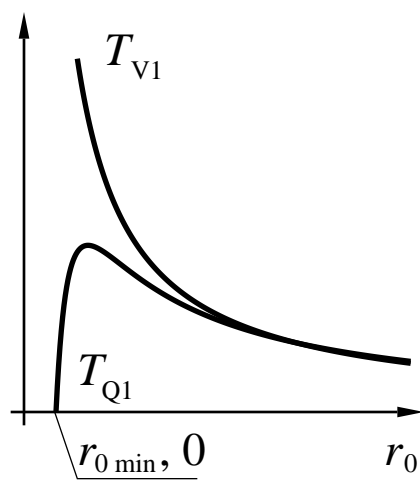


Fig. 6.

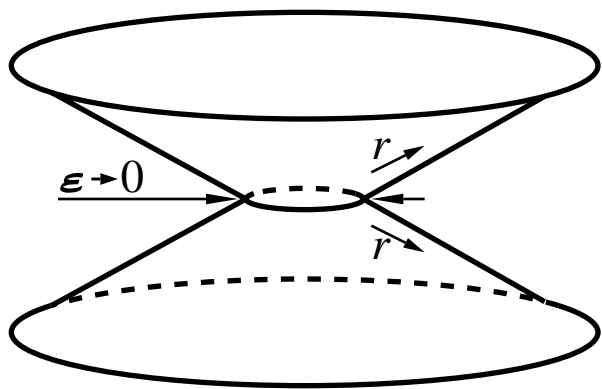


Fig. 7.

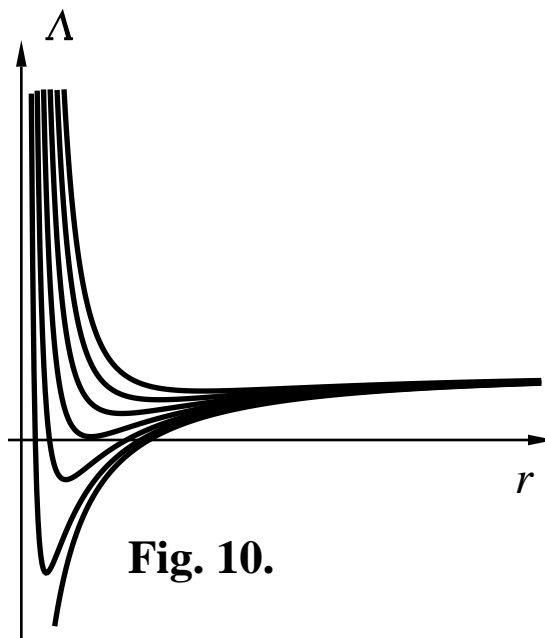


Fig. 10.

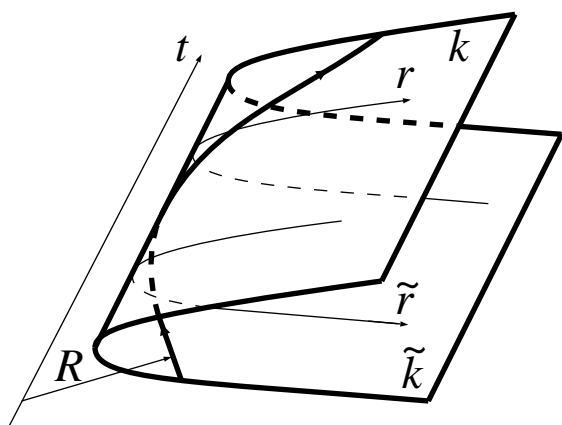


Fig. 8.

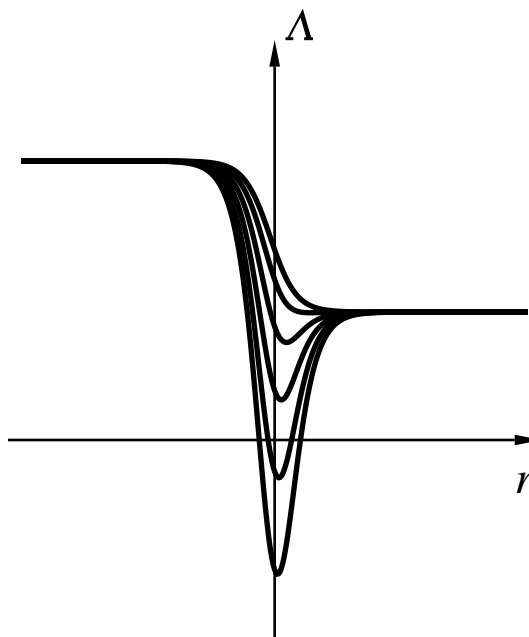


Fig. 11.

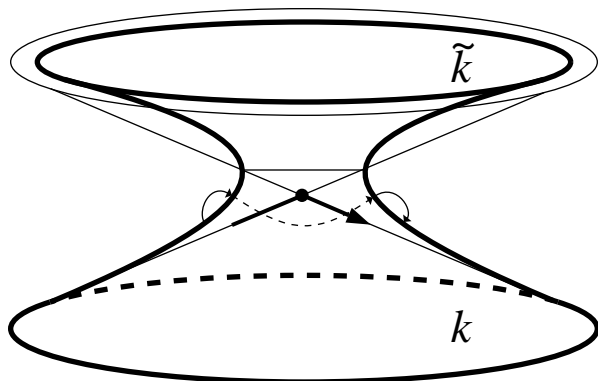


Fig. 9.